

Road Barlow Twins: Redundancy Reduction for Road Environment Descriptors and Motion Prediction

Royden Wagner

Karlsruhe Institute of Technology (KIT)
royden.wagner@kit.edu

Ömer Şahin Taş

FZI Research Center for Information Technology
tas@fzi.de

Marvin Klemp

Karlsruhe Institute of Technology (KIT)

Carlos Fernandez Lopez

Karlsruhe Institute of Technology (KIT)

Abstract: Anticipating the future motion of traffic agents is vital for self-driving vehicles to ensure their safe operation. We introduce a novel self-supervised pre-training method as well as a transformer model for motion prediction. Our method is based on Barlow Twins and applies the redundancy reduction principle to embeddings generated from HD maps. Additionally, we introduce a novel approach for redundancy reduction, where a potentially large and variable set of road environment tokens is transformed into a fixed-size set of road environment descriptors (RED). Our experiments reveal that the proposed pre-training method can improve minADE and minFDE by 12% and 15% and outperform contrastive learning with PreTraM and SimCLR in a semi-supervised setting. Our REDMotion model achieves results that are competitive with those of recent related methods such as MultiPath++ or Scene Transformer. Code is available at: <https://github.com/kit-mrt/road-barlow-twins>

Keywords: Transformers, self-supervised learning, pre-training, motion forecasting, trajectory prediction, self-driving, autonomous driving.

1 Introduction

It is essential for self-driving vehicles to understand the relation between the motion of traffic agents (such as other vehicles, pedestrians, and cyclists) and the surrounding road environment. Motion prediction aims to predict the future trajectory of traffic agents based on past trajectories and the given traffic scenario. Recent state-of-the-art methods for motion prediction (e.g., [1, 2, 3]) are deep learning methods trained using supervised learning. As the performance of deep learning methods scales well with the amount of training data [4, 5, 6], there is a great research interest in self-supervised learning methods, which generate supervisory signals from unlabeled data. While self-supervised methods are well established in the field of computer vision (e.g., [7, 8, 9]), their application to motion prediction in self-driving has only recently started to emerge (e.g., [10, 11]). One of the main reasons contributing to this is the limited availability and relatively small size of datasets for motion prediction in self-driving until recently (e.g., highD [12] 147 hours recorded vs. Woven Prediction dataset [13] 1001 hours recorded).

In this work, we focus on HD-map-assisted motion prediction and introduce a novel self-supervised pre-training method. Our method applies the redundancy reduction principle from Barlow Twins [14] to embeddings generated from HD maps. Through our method, deep learning models learn augmentation-invariant features of HD maps as pre-training. We hypothesize that by utilizing these features, relations in the road environment can be learned faster during subsequent fine-tuning.

We specifically target transformer models [15] for three reasons: (a) Transformers are successfully applied to a wide range of applications in natural language processing (e.g., [15, 16, 17]), computer

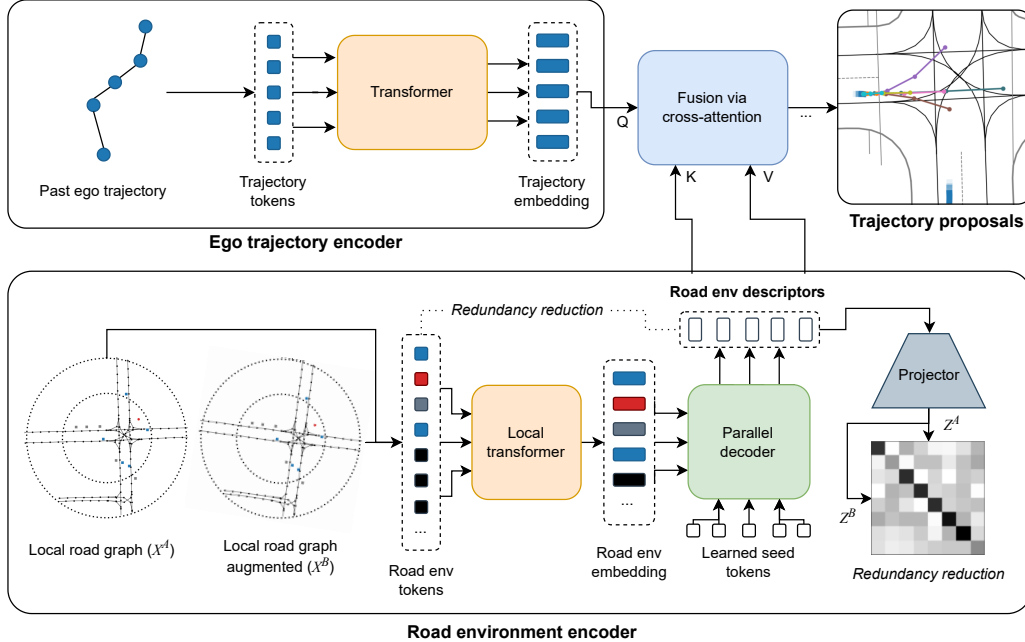


Figure 1: **REDMotion model**. Our model consists of two encoders. The ego trajectory encoder generates an embedding for the past trajectory of the ego agent. The road environment encoder generates a set of road environment descriptors as context embedding. Both embeddings are fused via cross-attention to yield trajectory proposals per agent.

vision (e.g., [18, 19, 20]), and time-series prediction (e.g., [21, 22]). Therefore, it is likely that enhancements in training mechanisms in a particular application will also apply to other applications. (b) Transformers have no inductive biases for generating features based on spatial correlations [23]. Therefore, appropriate mechanisms must be learned from data. (c) The performance of transformers on various downstream tasks scales very well with datasets [5, 6].

Our contributions are the following:

1. We propose a novel self-supervised pre-training objective for motion prediction.
2. We present a novel transformer model that generates road environment descriptors via redundancy reduction.
3. We introduce two vision transformer (ViT) based baseline models for motion prediction.
4. We evaluate various pre-training methods for motion prediction by comparing different models and dataset sizes.

2 Related Work

Recent works on motion prediction utilize a variety of deep learning model architectures, including transformers, graph-neural networks (GNNs), or convolutional neural networks (CNNs).

Ngiam et al. use PointNet [25] to encode polylines as a road graph. They fuse information from agent interactions across time steps and the road graph using attention mechanisms [24]. Nayakanti et al. combine early and late fusion with two basic primitives: a self-attention encoder and a cross-attention decoder. They investigate how to use a pure transformer without domain-specific modifications resulting in a motion prediction architecture that is similar to transformer architectures from other domains [3]. However, one drawback of this approach is that its internal mechanisms are less interpretable than other motion prediction models.

Gao et al. create vectorized HD-maps and agent trajectories and utilize a fully-connected homogeneous graph and inspect the scene from the viewpoint of every agent. For their homogeneous graph, they learn a node embedding for every object in the scene [26]. Later works utilizing GNNs use heterogeneous graphs [27, 28, 29]. Monninger et al. and Cui et al. highlight that choosing a fixed reference coordinate frame is vulnerable to domain shift and aim for viewpoint-invariant representation [27, 29]. These works store spatial information of lanes and agents in edges. Although GNN-based approaches are quite popular for interaction modeling, their scaling properties can be undesirable. Furthermore, they require additional modules to generate graph representations for multi-modal inputs.

CNN-based approaches have emerged as straightforward yet effective baselines in motion prediction. These approaches often employ a fixed CNN-head, with only the head being adapted to the specific requirements of the application. Recent works remain competitive in motion prediction benchmarks [30, 31]. However, CNN architectures typically tend to require larger models compared to GNNs due to the low information content per pixel. Additionally, they can capture interactions between entities only intrinsically.

Labeled data requirements of preceding approaches have motivated the application of self-supervised learning on motion prediction. PreTraM [10] exploits for contrastive pre-training that a traffic agent’s trajectory is correlated to the map. Inspired by CLIP [8], the similarity of embeddings generated from rasterized HD map images and past agent trajectories is maximized as pre-training. Therefore, past trajectories are required, which limits the application of this method to annotated datasets.

Ma et al. [32] improve modeling interactions between traffic agents via contrastive pre-training with SimCLR [7]. They rasterize images of intersecting agent trajectories and pre-train the corresponding module by maximizing the similarity of different views of the same trajectory intersection. Accordingly, only a small part of the motion prediction pipeline is pre-trained and annotations are required to determine the trajectory intersections.

Azevedo et al. use graph representations of HD maps to generate possible traffic agent trajectories [11]. Trajectories are generated based on synthetic speeds and the connectivity of the graph nodes. The pre-training objective is the same as for the subsequent fine-tuning: motion prediction. While this method is well adapted to motion prediction, it requires non-trivial modeling of agent positions and synthetic velocities when applied to non-annotated data.

Luo et al. fuse information from camera and LiDAR sensors for self-supervised motion prediction [33]. Their method exploits the structural consistency of LiDAR point clouds and cross-sensor motion regularization for motion prediction. Correspondingly, the application of this method requires datasets that contain both camera and LiDAR data.

3 Method

In this work, we propose a novel transformer model that generates road environment descriptors via redundancy reduction and two ViT-based baseline models for motion prediction. Furthermore, we introduce for all model types a pre-training objective to learn representations from HD maps in a self-supervised manner.

3.1 Road environment descriptor motion model

Our proposed road environment descriptor motion model (REDMotion) is a transformer model that utilizes the redundancy reduction principle [34, 14] to learn rich representations of road environments. Specifically, we implement two types of redundancy reduction:

(a) Reduction from a variable length and potentially large set of road environment tokens to a fixed set of road environment descriptors (RED). RED are a fixed sized set of tokens that represent agent and lane features (see input road environment encoder in Figure 1). To capture global context, i.e.,

environment and lane features, we use a global cross-attention mechanism between RED tokens and road environment tokens (see parallel decoder in Figure 1). Accordingly, every RED token can attend to every road environment token. The Wayformer [3] model employs a similar decoding mechanism. It uses learned seed tokens to decode a fixed set of trajectory proposals from a context embedding of variable length. Compared to Wayformer, RED offers more flexibility, as we can add different motion prediction heads on top. In this work, we utilize a multilayer perceptron (MLP) as the motion head.

(b) Redundancy reduction between embeddings generated from RED tokens (see the projector in Figure 1). This auxiliary training objective, Road Barlow Twins (RBT), is based on Barlow Twins [14], which aims to learn augmentation-invariant features via redundancy reduction. For each training sample (X^A in Figure 1) we generate an augmented view (X^B). We use uniform distributions to sample random rotation (max. $\pm 10^\circ$) and shift augmentations (max. $\pm 1m$). Afterwards, the local transformer and parallel decoder within the road environment encoder generate a set of RED tokens per input view. Finally, an MLP-based projector generates two embeddings (Z^A and Z^B) from the RED tokens. For the two embedding vectors, a cross-correlation matrix is created. The training objective is to approximate this cross-correlation matrix to the corresponding identity matrix, while reducing the redundancy between individual vector elements. By approximating the identity matrix, similar RED token sets are learned for similar road environments. The redundancy reduction mechanism prevents that multiple RED tokens to learn similar features of an environment, increasing diversity. The mentioned modules of the road environment encoder are shown with more details in Appendix A.

We generate road environment tokens for agents and lanes based on a local road graph (see Figure 1). In this local road graph, the ego agent is in the center and we consider lane nodes within a radius of 50 meters and agent nodes within 25 meters. As input for the road environment encoder, we use a list of these tokens sorted by token type, polyline, and distance to the ego agent. The road environment encoder learns a semantic embedding for each token type, which is concatenated with the position relative to the ego agent. Since local relations are especially important for processing lanes, we use local attention [35] layers. Compared to classical attention layers, these have a local attention mechanism within a limited window instead of a global attention mechanism. In addition to the focus on local relations, this reduces memory requirements and allows us to process long input sequences. Correspondingly, the receptive field of each token grows with an increasing number of local attention layers. Figure 2 shows how a polyline-like representation is built up for a traffic lane token. For a better illustration, Figure 2 shows an example of an attention window of 2 tokens per layer, in our model, we use an attention window size of 16 tokens. The polyline-like structures built in the local transformer are set in relation to all surrounding tokens in the parallel decoder of RED tokens. This is implemented by a global cross-attention mechanism from RED tokens to road env tokens (see Figure 4). Thus, global representation can be learned by RED tokens.

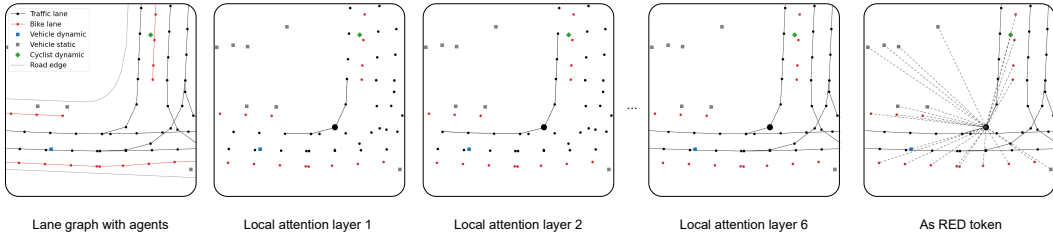


Figure 2: **Receptive field of a traffic lane token.** It expands with the increasing number of layers, thereby enabling the token to cover related tokens within a larger surrounding area. Consequently, the road environment tokens initially form a disconnected graph, but as the number of layers increases, they gradually transform into a fully connected graph.

In addition to the road environment, we encode the past trajectory of the ego agent with a standard transformer encoder (Ego trajectory encoder in Figure 1). The ego trajectory encoder learns a se-

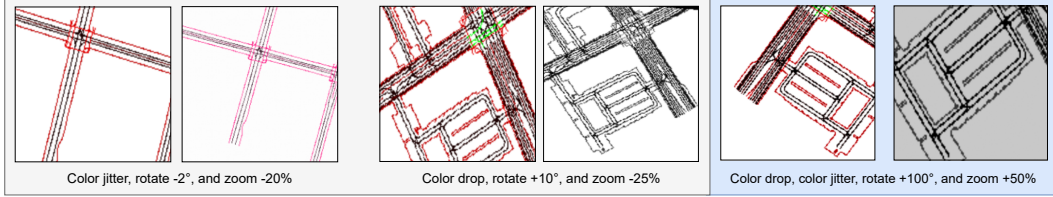


Figure 3: **Gray:** Proposed weaker augmentations for rasterized HD maps. **Blue:** Stronger vanilla Barlow Twins augmentations.

mantic embedding per agent type, which is concatenated with a temporal encoding and the position relative to the current position of the ego agent. As temporal encoding, we use the number of time steps between the encoded time step and the time step at which the prediction starts. The trajectory embedding is fused with RED tokens via cross-attention. Query vectors are generated from the trajectory embedding and key and value vectors from the RED tokens. Finally, we use global average pooling over the feature dimension to reduce the input dimension for an MLP based motion head. This MLP head regresses 6 trajectory proposals and the corresponding confidences per agent.

3.2 Baseline MotionViT models

We propose a baseline model similar to MotionCNN [30]. MotionCNN is a CNN for motion prediction that achieves competitive performance. Thus, it shares properties with ResNet-50 models [36], which are typically used to evaluate self-supervised methods in computer vision (e.g., [7, 14]). The model is composed of a CNN-backbone and a head with a single fully connected layer. As input, rasterized HD map images and rasterized past agent trajectories from the birds-eye view perspective are used. As output, six trajectory proposals and the associated confidences are predicted per traffic agent. All outputs are normalized with the softmax operator. For our first proposed architecture (MotionViT), we replace the CNN backbone in the model architecture with a vision transformer (ViT) [18]. Accordingly, the 224x224 pixel HD map images are split into 16x16 pixel patches and processed by a transformer encoder [15] along positional embeddings and a learned class token (cf. Figure 6). The class token learns a representation of the whole traffic scene as a combination of the patch tokens. Therefore, we use the class token as input for the motion head, which predicts the trajectory proposals.

Inspired by CLIP, we propose a second baseline model (DualMotionViT). The DualMotionViT architecture contains separate transformer encoders for map and agent data. The map and agent tokens, which are generated by the two encoders, are fused in an additional fusion block (cf. Figure 6). We use a memory efficient version of cross-attention [37] to fuse information from both token sets. In detail, the class token from the agent token set attends to the patch tokens of the map token set. Therefore, the computational complexity of the attention mechanism is reduced from $O(n^2)$ to $O(n)$, where n is the number of tokens in either set. Finally, the fused class token serves as input for the motion head.

For the two baseline models, we implement a similar form of RBT-pre-training as for the RED-Motion model. For this, we adapt the vanilla Barlow Twins augmentations for images to the new modality of HD-map raster images. We remove Gaussian blurring as our models will never process blurred HD map images during fine-tuning or inference for motion prediction. Furthermore, we remove image flipping and limit geometric transformations to moderate rotations (max. +/- 10°) and zooming (max. +/- 30%). The motivation for this is that geometrically highly modified maps should be interpreted differently during the fine-tuning process. Accordingly, the corresponding feature representations should be different as well. Additionally, we use color jitter and color drop as augmentation. Figure 3 shows examples of the augmentations we use and the stronger vanilla Barlow Twins augmentations.

4 Results

4.1 Comparing pre-training methods for motion prediction

In this set of experiments, we compare our proposed pre-training method with contrastive learning. As examples of contrastive learning, we use two configurations of PreTraM and the vanilla SimCLR. The first configuration of PreTraM is a combination of map contrastive learning (MCL) via SimCLR and trajectory-map contrastive learning (TMCL). For TMCL, the similarity of embeddings from map data and past agent trajectories of the same scene is maximized. As the second configuration of PreTraM, we evaluate TMCL without MCL. Comparable to MotionCNN, which is pre-trained on ImageNet, we additionally evaluate a combination of our method and ImageNet pre-training. In this case, we initialize the ViT-L model with ImageNet weights before pre-training with our method.

Dataset. We use the official training and validation splits of the Waymo Open Motion dataset [38] as training and validation data. Correspondingly, 100% of the training split is 2.2M agent related training samples. Since pre-training is particularly useful when little annotated data is available, we reduce the training dataset in this experiment to 12.5% and 3.75%. Validation and evaluation are performed on 200K samples. In addition to the map, the trajectories of all traffic agents from the last second are used as input during fine-tuning for motion prediction. The data set is sampled with 10 Hz, accordingly 10 time points are used as input.

Evaluation metrics. We use the L5Kit [13] to evaluate the multimodal trajectory predictions of our models. Following common practice [13, 38], we use the final displacement error (FDE) and the average displacement error (ADE) to evaluate trajectory proposals. The ADE and FDE scores are evaluated in the oracle/minimum mode. Accordingly, the distance errors of the trajectory proposal with the lowest distance error are measured. minADE and minFDE metrics are computed at different prediction horizons of 3s and 5s and averaged. Additionally, we introduce the $\Delta\text{minADE}_{\text{rel}}$ and $\Delta\text{minFDE}_{\text{rel}}$ scores, which measure the relative change w.r.t. the baselines without pre-training. Accordingly, the $\Delta\text{minADE}_{\text{rel}}$ is computed with

$$\Delta\text{minADE}_{\text{rel}} = \frac{\text{minADE}_{\text{pre}} - \text{minADE}_{\text{base}}}{\text{minADE}_{\text{base}}} \cdot 100. \quad (1)$$

T_{rel} measures the relative change in training time w.r.t. the baselines. f_{ds} is the fraction of training data used.

Experimental setup. For TMCL pre-training, we use the dataset without trajectory labels. For the RBT, MCL, and SimCLR pre-training, we use the same dataset, but remove all data related to traffic agents. For all three methods and backbone models, we add a projection head with 3 fully connected layers. The first layer has 1024 nodes, the following two layers have 2048 nodes. The training samples are augmented using the weaker augmentations shown in Figure 3. For the DualMotionViT models, we use two ViT-B/16 models as map and agent encoders. For pre-training and fine-tuning, we use AdamW [39] as the optimizer. The initial learning rate is set to 10^{-4} and reduced to 10^{-6} using a cosine annealing learning rate scheduler. As fine-tuning loss, we are minimizing the negative multivariate log-likelihood loss.

Results. Table 1 shows the results of this experiment. When fine-tuning on 12.5% of the training split, our pre-training method improves the minADE score by 12% and the minFDE score by 15% compared to the baseline without pre-training. Contrastive pre-training performs worst in this setup. We hypothesize that this is due to the fact that augmented views of different HD maps are still rather similar to each other compared to images of different classes in ImageNet (e.g., cars and birds). During contrastive pre-training, all samples in a batch other than the current one are treated as negative examples. Therefore, the pre-training objective becomes to learn dissimilar embeddings for rather similar samples. Initializing the model with weights learned from training on ImageNet worsens the performance as well. This highlights the domain gap between general purpose vision datasets and motion prediction datasets with HD maps. This gap also seems to have a stronger impact on our architecture than, for example, on MotionCNN. One possible interpretation is that the learned feature extraction mechanisms in a ViT adapt more to the training data than in CNNs [23].

Model	Pre-training	Config	f_{ds}	minFDE ↓	Δ minFDE _{rel}	minADE ↓	Δ minADE _{rel}	T_{rel}	#Params
MotionViT	None		12.5%	<u>1.865</u>		<u>0.794</u>		1.0	310M
	RBT (ours)		12.5%	1.584	-15.07%	0.697	-12.22%	2.0	310M
	SimCLR [7]		12.5%	2.483	+33.14%	1.172	+47.61%	2.0	310M
	RBT	+ ImageNet	12.5%	2.297	+23.16%	0.942	+18.64%	2.0	310M
MotionViT	None		3.75%	<u>2.554</u>		<u>1.096</u>		1.0	310M
	RBT (ours)		3.75%	2.552	-0.08%	<u>87.8</u>	-0.64%	2.0	310M
	SimCLR [7]		3.75%	11.494	+350.04%	2.921	+166.51%	2.0	310M
	RBT	+ ImageNet	3.75%	2.602	+1.88%	1.107	+1.00%	2.0	310M
DualMotionViT	None		12.5%	1.672		0.723		1.0	190M
	RBT (ours)		12.5%	<u>1.565</u>	-6.40%	<u>0.691</u>	-4.43%	2.0	190M
	PreTraM [10]	MCL + TMCL	12.5%	1.643	-1.73%	0.718	-0.69%	2.0	190M
	PreTraM [10]	TMCL (our)	12.5%	1.529	-8.55%	0.679	-6.09%	2.0	190M
REDMotion	None		12.5%	1.494		<u>0.717</u>		1.0	26M
	RBT (ours)	RBT-aux	12.5%	<u>1.402</u>	-6.16%	<u>0.739</u>	+3.07%	1.0	26M
	RBT (ours)	RBT-aux	100%	1.099	-26.44%	0.534	-25.52%	4.0	26M

Table 1: **Comparing pre-training methods using different models and dataset sizes.** Best scores are bold, second best are underlined.

Fine-tuning on 3.75% of the training split yields similar results, but the differences in performance are less significant and all methods perform worse. This could be due to the fact that our pre-training method learns useful feature extraction mechanisms only for environment perception. However, for motion prediction, the information about traffic agents is crucial. This needs to be learned by a large transformer model, for which sufficient data is needed.

The third block in Table 1 shows the results achieved with the DualMotionViT model. Already without pre-training, 10% lower minADE and 9% lower minFDE values are achieved than with the MotionViT model. The DualMotionViT model also requires 120M fewer parameters to achieve these values. This shows that it is advantageous for motion prediction to first process map and agent data individually and then merge them in the embedding space. Our pre-training method can reduce the minADE and minFDE values by a further 4% and 6% respectively. Vanilla PreTraM with MCL and TMCL improves the minADE and minFDE scores only by 1% and 2%. Therefore, our method can outperform vanilla PreTraM in this semi-supervised setting. Overall, however, our new variation of PreTraM without MCL performs best in this experiment.

For both baseline models, the training time with pre-training is twice as long as without ($T_{rel} = 2.0$), since we perform pre-training and fine-tuning for the same amount of time.

The fourth block in Table 1 shows the results of our new REDMotion model, which uses vector representations as input tokens instead of image patches. Without pre-training, this model achieves 11% lower minFDE scores compared to the DualMotionViT model. With 26M parameters, this model also requires 86% fewer parameters. With the auxiliary RBT loss, the minFDE score improves by 6%, the minADE score worsens by 3%. Table 3 shows the minFDE and minADE scores of our model per agent class. Figure 7 shows some additional qualitative results of our REDMotion model. A significant advantage of the auxiliary loss is that it acts as additional regularization during training. Figure 5 ((a) vs. (b)) shows how this reduces the difference between training and validation loss towards the end of the training. Moreover, the auxiliary RBT loss does not increase the training time ($T_{rel} = 1.0$), since it is minimized together with the motion prediction loss. Therefore, we also use this loss to train the REDMotion model on the entire dataset. The last row shows that the performance scales with the dataset and again 20% lower minFDE scores and 29% lower minADE scores are achieved.

4.2 Comparing motion prediction models

In this experiment, we compare our best model, REDMotion, with other recent models for motion prediction. We do not use ensembling for our model, therefore we compare our model with the best single model version of the other approaches.

Dataset. We use 100% of the Waymo Open Motion training set for training to compare the performance of our model with that of other recent models. We perform evaluation on the validation split.

Evaluation metrics. We use the same metrics for trajectories as in the previous experiment. However, this time, as in the Waymo Open Motion Challenge [38], the minFDE and minADE scores are computed for three prediction horizons of 3s, 5s, and 8s and then averaged. Additionally, we report the minFDE and minADE scores for the prediction horizon of 8s.

Results. Table 2 shows the performance of our model in comparison to other motion prediction models. Our proposed model can outperform both MotionCNN variants and the joint prediction version of Scene Transformer in terms of minFDE and minADE scores. Overall, the marginal prediction version of the Scene Transformer achieves the lowest minFDE and minADE scores. For the minFDE @8s metric, our model ranks second behind the marginal prediction version of the Scene Transformer. For the minADE @8s metric, our model ranks third behind the marginal prediction version of Scene Transformer and MultiPath++.

Model	minFDE ↓	minADE ↓	minFDE @8s ↓	minADE @8s ↓
MotionCNN ResNet18 [30]	1.640	0.815	-	-
MotionCNN Xception [30]	1.496	0.738	-	-
MultiPath [40]	-	-	4.752	1.796
MultiPath++ [31]	-	-	2.305	0.978
Scene Transformer (marginal) [24]	1.220	0.613	2.070	0.970
Scene Transformer (joint) [24]	1.804	0.837	3.113	1.353
REDMotion (ours)	<u>1.409</u>	<u>0.736</u>	<u>2.210</u>	1.211

Table 2: **Comparing motion prediction models.** Best scores are bold, second best are underlined.

5 Limitations

We use a world on rails assumption [41] for our model and predict trajectories marginally. Accordingly, we predict the trajectory of each agent in a scene individually without considering the predicted trajectories of the surrounding agents. In theory, better predictions can be made by joint prediction. However, the worse performance of the Scene Transformer (see Table 2) in the joint configuration shows, for example, that in common benchmarks the performance can also be worsened by joint prediction.

6 Contribution and Future Work

In this work, we introduced a novel self-supervised pre-training method for motion prediction in the field of autonomous driving. Our approach builds upon Barlow Twins and learns augmentation-invariant features of HD maps. Unlike similar methods, our approach eliminates the need for traffic agent annotations and offers end-to-end training. Our evaluations indicate that this pre-training method can improve the accuracy of motion prediction and outperform contrastive learning approaches. Furthermore, we presented two new transformer-based models that serve as baselines for motion prediction and a novel transformer model that generates road environment descriptors (RED) via redundancy reduction. The method for creating RED provides a universal approach to perform redundancy reduction, transforming a context of variable length into a fixed size embedding. The corresponding REDMotion model attains results that are competitive with those of state-of-the-art methods. In future work, this approach can be applied to other context representations, extending to other multi-modal inputs beyond agent and map data.

References

- [1] S. Shi, L. Jiang, D. Dai, and B. Schiele. Motion transformer with global intention localization and local movement refinement. In *36th Conference on Neural Information Processing Systems*, 2022.
- [2] J. Gu, C. Sun, and H. Zhao. Densetnt: End-to-end trajectory prediction from dense goal sets. In *Proceedings of the IEEE/CVF International Conference on Computer Vision*, pages 15303–15312, 2021.
- [3] N. Nayakanti, R. Al-Rfou, A. Zhou, K. Goel, K. S. Refaat, and B. Sapp. Wayformer: Motion forecasting via simple & efficient attention networks. In *IEEE International Conference on Robotics and Automation (ICRA)*, 2023.
- [4] C. Sun, A. Shrivastava, S. Singh, and A. Gupta. Revisiting unreasonable effectiveness of data in deep learning era. In *Proceedings of the IEEE international conference on computer vision*, pages 843–852, 2017.
- [5] J. Kaplan, S. McCandlish, T. Henighan, T. B. Brown, B. Chess, R. Child, S. Gray, A. Radford, J. Wu, and D. Amodei. Scaling laws for neural language models. *arXiv preprint arXiv:2001.08361*, 2020.
- [6] X. Zhai, A. Kolesnikov, N. Houlsby, and L. Beyer. Scaling vision transformers. In *Proceedings of the IEEE/CVF Conference on Computer Vision and Pattern Recognition*, pages 12104–12113, 2022.
- [7] T. Chen, S. Kornblith, M. Norouzi, and G. Hinton. A simple framework for contrastive learning of visual representations. In *International conference on machine learning*, pages 1597–1607. PMLR, 2020.
- [8] A. Radford, J. W. Kim, C. Hallacy, A. Ramesh, G. Goh, S. Agarwal, G. Sastry, A. Askell, P. Mishkin, J. Clark, et al. Learning transferable visual models from natural language supervision. In *International conference on machine learning*, pages 8748–8763. PMLR, 2021.
- [9] K. He, H. Fan, Y. Wu, S. Xie, and R. Girshick. Momentum contrast for unsupervised visual representation learning. In *Proceedings of the IEEE/CVF conference on computer vision and pattern recognition*, pages 9729–9738, 2020.
- [10] C. Xu, T. Li, C. Tang, L. Sun, K. Keutzer, M. Tomizuka, A. Fathi, and W. Zhan. Pretram: Self-supervised pre-training via connecting trajectory and map. In *Computer Vision–ECCV 2022: 17th European Conference, Tel Aviv, Israel, October 23–27, 2022, Proceedings, Part XXXIX*, pages 34–50. Springer, 2022.
- [11] C. Azevedo, T. Gilles, S. Sabatini, and D. Tsishkou. Exploiting map information for self-supervised learning in motion forecasting. *arXiv preprint arXiv:2210.04672*, 2022.
- [12] R. Krajewski, J. Bock, L. Kloeker, and L. Eckstein. The highd dataset: A drone dataset of naturalistic vehicle trajectories on german highways for validation of highly automated driving systems. In *2018 21st International Conference on Intelligent Transportation Systems (ITSC)*, pages 2118–2125. IEEE, 2018.
- [13] J. Houston, G. Zuidhof, L. Bergamini, Y. Ye, L. Chen, A. Jain, S. Omari, V. Iglovikov, and P. Ondruska. One thousand and one hours: Self-driving motion prediction dataset. In *Conference on Robot Learning*, pages 409–418. PMLR, 2021.
- [14] J. Zbontar, L. Jing, I. Misra, Y. LeCun, and S. Deny. Barlow twins: Self-supervised learning via redundancy reduction. In *International Conference on Machine Learning*, pages 12310–12320. PMLR, 2021.

- [15] A. Vaswani, N. Shazeer, N. Parmar, J. Uszkoreit, L. Jones, A. N. Gomez, Ł. Kaiser, and I. Polosukhin. Attention is all you need. *Advances in neural information processing systems*, 30, 2017.
- [16] T. Brown, B. Mann, N. Ryder, M. Subbiah, J. D. Kaplan, P. Dhariwal, A. Neelakantan, P. Shyam, G. Sastry, A. Askell, et al. Language models are few-shot learners. *Advances in neural information processing systems*, 33:1877–1901, 2020.
- [17] OpenAI. Gpt-4 technical report, 2023.
- [18] A. Dosovitskiy, L. Beyer, A. Kolesnikov, D. Weissenborn, X. Zhai, T. Unterthiner, M. Dehghani, M. Minderer, G. Heigold, S. Gelly, et al. An image is worth 16x16 words: Transformers for image recognition at scale. In *International Conference on Learning Representations*.
- [19] N. Carion, F. Massa, G. Synnaeve, N. Usunier, A. Kirillov, and S. Zagoruyko. End-to-end object detection with transformers. In *Computer Vision—ECCV 2020: 16th European Conference, Glasgow, UK, August 23–28, 2020, Proceedings, Part I 16*, pages 213–229. Springer, 2020.
- [20] T. Meinhardt, A. Kirillov, L. Leal-Taixe, and C. Feichtenhofer. Trackformer: Multi-object tracking with transformers. In *Proceedings of the IEEE/CVF conference on computer vision and pattern recognition*, pages 8844–8854, 2022.
- [21] H. Zhou, S. Zhang, J. Peng, S. Zhang, J. Li, H. Xiong, and W. Zhang. Informer: Beyond efficient transformer for long sequence time-series forecasting. In *Proceedings of the AAAI conference on artificial intelligence*, volume 35, pages 11106–11115, 2021.
- [22] T. Zhou, Z. Ma, Q. Wen, X. Wang, L. Sun, and R. Jin. Fedformer: Frequency enhanced decomposed transformer for long-term series forecasting. In *International Conference on Machine Learning*, pages 27268–27286. PMLR, 2022.
- [23] M. Raghu, T. Unterthiner, S. Kornblith, C. Zhang, and A. Dosovitskiy. Do vision transformers see like convolutional neural networks? *Advances in Neural Information Processing Systems*, 34:12116–12128, 2021.
- [24] J. Ngiam, B. Caine, V. Vasudevan, Z. Zhang, H. L. Chiang, J. Ling, R. Roelofs, A. Bewley, C. Liu, A. Venugopal, D. Weiss, B. Sapp, Z. Chen, and J. Shlens. Scene transformer: A unified architecture for predicting multiple agent trajectories. In *International Conference on Learning Representations*, 2022.
- [25] C. R. Qi, H. Su, K. Mo, and L. J. Guibas. Pointnet: Deep learning on point sets for 3d classification and segmentation. In *Proceedings of the IEEE conference on computer vision and pattern recognition*, pages 652–660, 2017.
- [26] J. Gao, C. Sun, H. Zhao, Y. Shen, D. Anguelov, C. Li, and C. Schmid. Vectornet: Encoding hd maps and agent dynamics from vectorized representation. In *Proceedings of the IEEE/CVF Conference on Computer Vision and Pattern Recognition*, pages 11525–11533, 2020.
- [27] T. Monninger, J. Schmidt, J. Rupprecht, D. Raba, J. Jordan, D. Frank, S. Staab, and K. Dietmayer. Scene: Reasoning about traffic scenes using heterogeneous graph neural networks. *IEEE Robotics and Automation Letters*, 2023.
- [28] D. Grimm, P. Schörner, M. Dreßler, J. Zöllner, et al. Holistic graph-based motion prediction. 2023.
- [29] A. Cui, S. Casas, K. Wong, S. Suo, and R. Urtasun. Gorela: Go relative for viewpoint-invariant motion forecasting. In *IEEE International Conference on Robotics and Automation (ICRA)*, 2023.
- [30] S. Konev, K. Brodt, and A. Sanakoyeu. Motioncnn: a strong baseline for motion prediction in autonomous driving. *arXiv preprint arXiv:2206.02163*, 2022.

- [31] B. Varadarajan, A. Hefny, A. Srivastava, K. S. Refaat, N. Nayakanti, A. Cornman, K. Chen, B. Douillard, C. P. Lam, D. Anguelov, et al. Multipath++: Efficient information fusion and trajectory aggregation for behavior prediction. In *2022 International Conference on Robotics and Automation (ICRA)*, pages 7814–7821. IEEE, 2022.
- [32] H. Ma, Y. Sun, J. Li, and M. Tomizuka. Multi-agent driving behavior prediction across different scenarios with self-supervised domain knowledge. In *2021 IEEE International Intelligent Transportation Systems Conference (ITSC)*, pages 3122–3129. IEEE, 2021.
- [33] C. Luo, X. Yang, and A. Yuille. Self-supervised pillar motion learning for autonomous driving. In *Proceedings of the IEEE/CVF Conference on Computer Vision and Pattern Recognition*, pages 3183–3192, 2021.
- [34] H. Barlow. Redundancy reduction revisited. *Network: computation in neural systems*, 12(3): 241, 2001.
- [35] I. Beltagy, M. E. Peters, and A. Cohan. Longformer: The long-document transformer. *arXiv preprint arXiv:2004.05150*, 2020.
- [36] K. He, X. Zhang, S. Ren, and J. Sun. Deep residual learning for image recognition. In *Proceedings of the IEEE conference on computer vision and pattern recognition*, pages 770–778, 2016.
- [37] C.-F. R. Chen, Q. Fan, and R. Panda. Crossvit: Cross-attention multi-scale vision transformer for image classification. In *Proceedings of the IEEE/CVF international conference on computer vision*, pages 357–366, 2021.
- [38] S. Ettinger, S. Cheng, B. Caine, C. Liu, H. Zhao, S. Pradhan, Y. Chai, B. Sapp, C. R. Qi, Y. Zhou, et al. Large scale interactive motion forecasting for autonomous driving: The waymo open motion dataset. In *Proceedings of the IEEE/CVF International Conference on Computer Vision*, pages 9710–9719, 2021.
- [39] I. Loshchilov and F. Hutter. Decoupled weight decay regularization. In *International Conference on Learning Representations*, 2019.
- [40] Y. Chai, B. Sapp, M. Bansal, and D. Anguelov. Multipath: Multiple probabilistic anchor trajectory hypotheses for behavior prediction. In *Conference on Robot Learning*, pages 86–99. PMLR, 2020.
- [41] D. Chen, V. Koltun, and P. Krähenbühl. Learning to drive from a world on rails. In *IEEE/CVF International Conference on Computer Vision (ICCV)*, pages 15590–15599, 2021.

7 Appendix

A Road environment encoder in detail

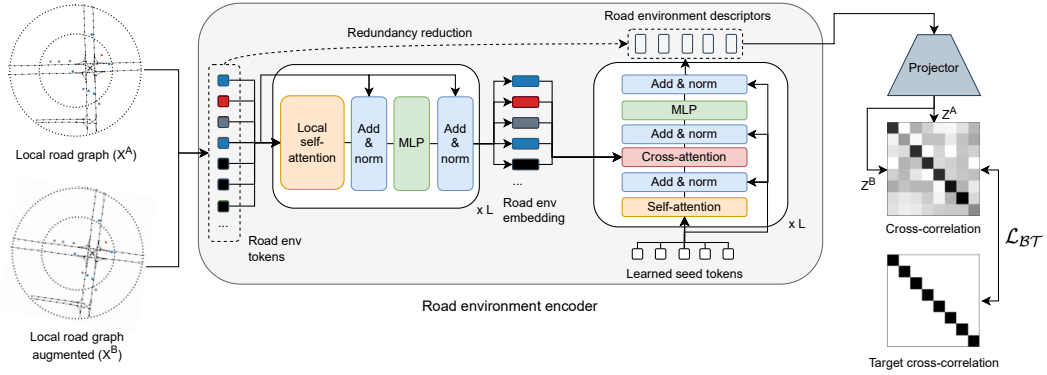


Figure 4: Road environment encoder. \mathcal{L}_{BT} is the Barlow Twins loss, L is the number of modules.

B Training dynamics

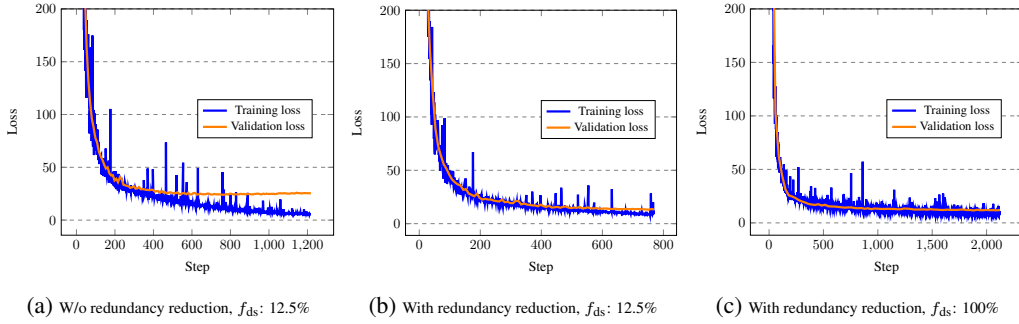


Figure 5: Training dynamics with and without auxiliary redundancy reduction

C Baseline models in detail

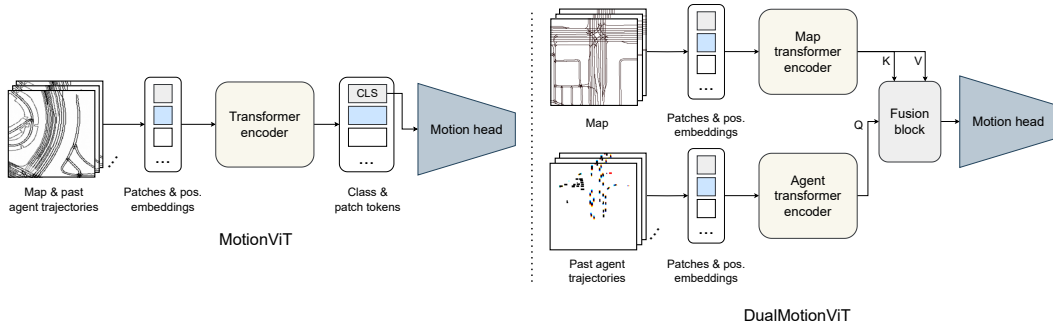


Figure 6: Proposed baseline models. **MotionViT:** A shared transformer encoder to encode both map data and past agent trajectories. **DualMotionViT:** Separate transformer encoders for map and agent data. Generated embeddings are fused via cross-attention (Queries Q , Keys K , and Values V).

D Quantitative results per agent class

Agent class	minFDE @ 3s ↓	minADE @ 3s ↓	minFDE @ 5s ↓	minADE @ 5s ↓
Vehicle	0.804	0.411	2.039	0.929
Pedestrian	0.375	0.195	0.803	0.391
Cyclist	0.814	0.424	1.759	0.852

Table 3: Prediction performance of our REDMotion model per agent class

E Qualitative results

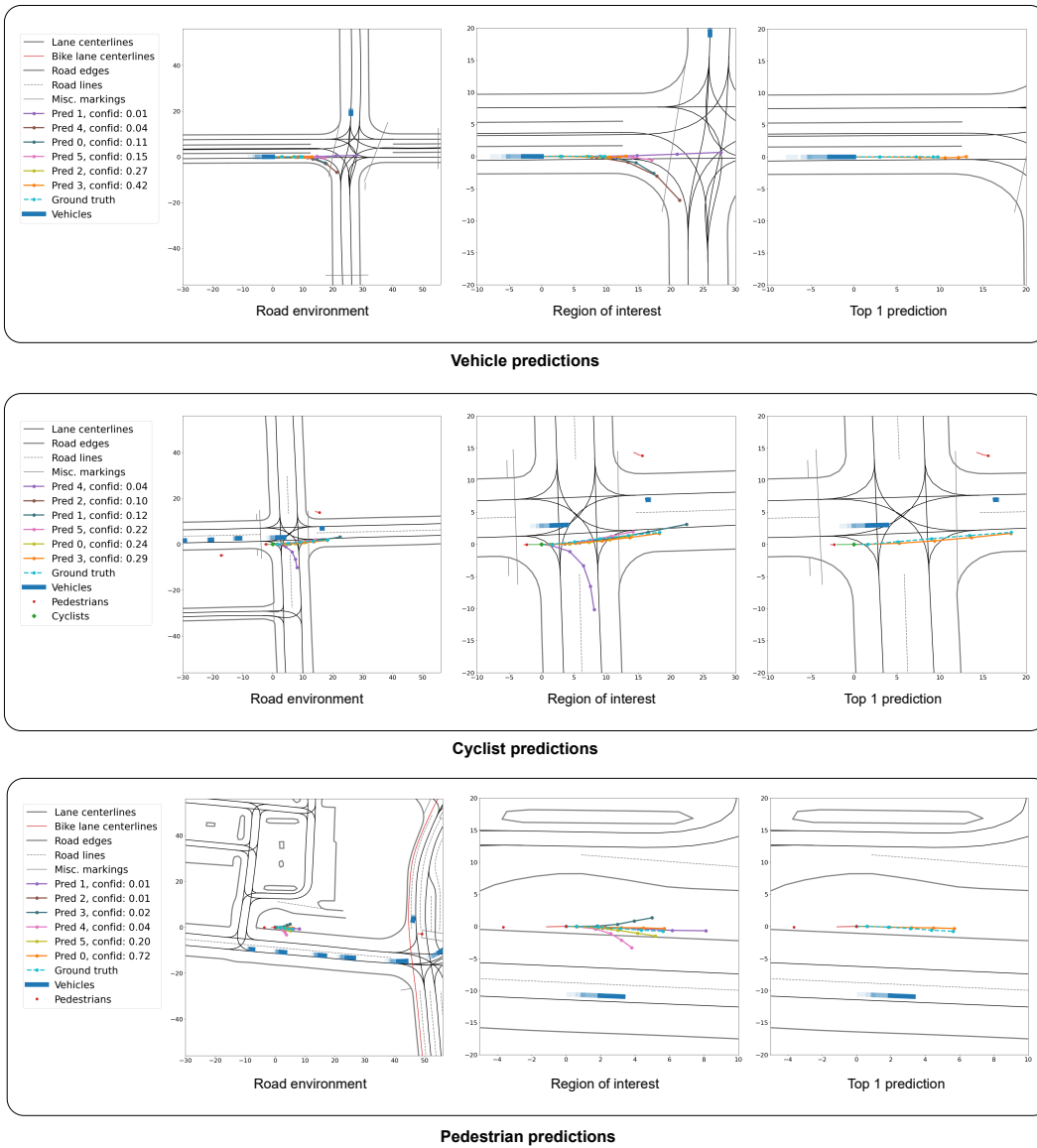


Figure 7: **Trajectory proposals of our REDMotion model.** Past trajectories of traffic agents are visualized with decreasing opacity, the ground truth future trajectory as cyan blue lines, and the trajectory proposals of our model are in decreasing order of confidence scores: orange, green, pink, dark blue, brown, and violet. Discrete predicted agent locations are marked as dots. x and y axes ticks are in meters. Best viewed zoomed in.